

# Strongly polarizing weakly coupled $^{13}\text{C}$ nuclear spins with optically pumped nitrogen-vacancy center

Ping Wang

*Hefei National Laboratory for Physics Sciences at Microscale and Department of Modern Physics,  
University of Science and Technology of China, Hefei, Anhui 230026, China and  
Beijing Computational Science Research Center, Beijing 100084, China*

Bao Liu and Wen Yang\*

*Beijing Computational Science Research Center, Beijing 100084, China*

(Dated: April 29, 2019)

Enhancing the polarization of nuclear spins surrounding the nitrogen-vacancy (NV) center in diamond has attracted widespread attention recently due to its various applications. Here we present an analytical theory and comprehensive understanding on how to optimize the dynamic nuclear polarization by an optically pumped NV center near the ground state level anticrossing. Our results not only provide a parameter-free explanation and a clearly physics picture for the recently observed polarization dependence on the magnetic field for strongly coupled  $^{13}\text{C}$  nuclei [H. J. Wang *et al.*, Nat. Commun. 4, 1 (2013)], but also demonstrate the possibility to strongly polarize weakly coupled  $^{13}\text{C}$  nuclei under weak optical pumping and suitably chosen magnetic field. This allows sensitive magnetic control of the  $^{13}\text{C}$  nuclear spin polarization for NMR applications and significant suppression of the  $^{13}\text{C}$  nuclear spin noise to prolong the NV spin coherence time.

## INTRODUCTION

The atomic nuclear spins are central elements for NMR and magnetic resonance imaging<sup>1</sup> and promising candidates for storing and manipulating long-lived quantum information<sup>2</sup> due to their long coherence time. However, the tiny magnetic moment of the nuclear spins makes them completely random in thermal equilibrium, even in a strong magnetic field and at low temperature. This poses severe limitations on their applications. The dynamic nuclear polarization (DNP) technique can bypass this limitation by transferring the electron spin polarization to the nuclear spins via the hyperfine interaction (HFI), but efficient DNP is usually prohibited at room temperature.

An exception is the negatively charged nitrogen-vacancy (NV) center<sup>3</sup> in diamond, which has an optically polarizable spin-1 electronic ground state with a long coherence time<sup>4</sup>, allowing DNP at room temperature<sup>5,6</sup>. This prospect has attracted widespread interest due to its potential applications in room-temperature NMR, magnetic resonance imaging and magnetometry<sup>7,8</sup>, electron-nuclear hybrid quantum register<sup>9-11</sup>, and electron spin coherence protection by suppressing the nuclear spin noise<sup>12</sup>. In addition to the remarkable success in coherently driving spectrally resolved transitions to initialize, manipulate, and readout up to three strongly coupled nuclear spins<sup>10,13-16</sup>, there are intense activities aiming to enhance the polarization of many nuclear spins via dissipative spin transfer from the NV to the nuclear spins. To overcome the large energy mismatch for resonant spin transfer, various strategies have been explored, e.g., tuning the NV spin near the excited state level anticrossing<sup>6,17-22</sup> or ground state level anticrossing (GSLAC)<sup>5,23,24</sup>, driving the NV-nuclear spins into Hartman-Hahn resonance<sup>25,26</sup> or selectively driving certain spectrally resolved transitions between hyperfine-mixed states under optical illumination<sup>27,28</sup>. Successful polarization of bulk nuclear spins in diamond have

dramatically enhanced the NMR signal by up to five orders of magnitudes<sup>17,28</sup> and significantly prolonged the NV spin coherence time<sup>25,26</sup>.

In particular, near NV excited state level anticrossing, almost complete polarization has been achieved for  $^{15}\text{N}$  (or  $^{14}\text{N}$ ) and  $^{13}\text{C}$  nuclei in the first shell of the vacancy<sup>6,20-22,29</sup>. Recently, Wang *et al.*<sup>24</sup> exploited the GSLAC to achieve near complete polarization of first-shell  $^{13}\text{C}$  nuclei and revealed multiple polarization sign reversals over a narrow range (a few mT) of magnetic field. This behavior has been attributed to the anisotropic HFI and could allow sensitive magnetic control of  $^{13}\text{C}$  nuclear spin polarization, but a clear understanding remains absent. Furthermore, in most of the existing works, only a few strongly coupled nuclear spins (HFI  $\gg$  200 kHz) are significantly polarized via direct spin transfer from the NV center, while many weakly coupled nuclear spins are only slightly polarized via nuclear spin diffusion. Enhancing the polarization of these weakly coupled nuclear spins could further improve NMR and magnetic resonance imaging<sup>17,27,28</sup> and prolong the NV spin coherence time<sup>25,26</sup>.

In this paper we present an analytical formula and a comprehensive understanding on how to optimize the DNP by an optically pumped NV center near the GSLAC at ambient temperature. Our results provide a parameter-free explanation and a clear physics picture for the experimentally observed magnetic field dependence of  $^{13}\text{C}$  nuclear polarization<sup>24</sup>. More importantly, we demonstrate the possibility to greatly enhance this magnetic field dependence and strongly polarize weakly coupled  $^{13}\text{C}$  nuclei (with HFI down to  $\sim$  1 kHz) via direct, resonant spin transfer under suitable conditions. First, we introduce our model and an intuitive picture for manipulating the DNP with an optically pumped NV center. Then we present our theory and analytical formula for the DNP of a single nuclear spin, which reveals the possibility of strongly polarizing weakly coupled nuclear spins under weak optical pumping and fine-tuned magnetic field. Finally, we demonstrate this possibility for multiple nuclear spins by providing

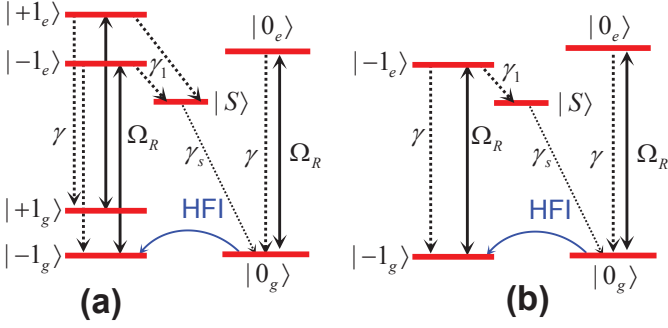


FIG. 1. (a) NV states at ambient temperature responsible for DNP under optical pumping. (b) Reduced five-level model for DNP near the ground state anticrossing.

a multi-spin DNP theory and its numerical solution.

## RESULTS

### Model and intuitive physics picture

First we briefly introduce our theoretical model, consisting of a negatively charged NV center coupled to many surrounding nuclear spins at ambient temperature. The NV center has a ground state triplet  $|\pm 1_g\rangle$  and  $|0_g\rangle$  separated by zero-field splitting  $D_{gs} = 2.87$  GHz and an excited state triplet  $|\pm 1_e\rangle$  and  $|0_e\rangle$  separated by zero-field splitting  $D_{es} = 1.41$  GHz<sup>29</sup>. In a magnetic field  $B$  along the N-V axis ( $z$  axis), the electron Zeeman splitting  $\gamma_e B$  with  $\gamma_e = 28.025$  GHz/T cancels the ground state zero-field splitting at a critical magnetic field  $D_{gs}/\gamma_e \approx 102$  mT, leading to GSLAC between  $|0_g\rangle$  and  $|-1_g\rangle$ . The GSLAC reduces the energy mismatch for the NV-nuclei flip-flop dynamics and enables NV-induced DNP through their HFI  $\hat{H}_{HF} = \sum_i \hat{\mathbf{F}}_i \cdot \hat{\mathbf{I}}_i$ , where  $\hat{\mathbf{F}}_i \equiv \hat{\mathbf{S}}_g \cdot \mathbf{A}_{g,i} + \hat{\mathbf{S}}_e \cdot \mathbf{A}_{e,i}$  is the electron Knight field coupled to the  $i$ th nucleus, and  $\hat{\mathbf{S}}_g$  ( $\hat{\mathbf{S}}_e$ ) is the NV ground (excited) state spin. The HFI tensors  $\mathbf{A}_{g,i}$  and  $\mathbf{A}_{e,i}$  are well established for the on-site nitrogen nucleus<sup>30</sup> and the nearest <sup>13</sup>C nuclear spins in the first shell of the vacancy<sup>19,31–33</sup>. For other <sup>13</sup>C nuclei, especially those  $> 6.3$  Å away from the NV center, very little information is available<sup>22,32–34</sup> and dipolar HFI is usually assumed<sup>25,26,35–37</sup>.

Next we provide an intuitive physics picture for engineering the DNP by controlling the NV center near the GSLAC. For brevity we focus on one nuclear spin- $I$  (e.g.,  $I = 1/2$  for the <sup>13</sup>C or <sup>15</sup>N nucleus and  $I = 1$  for the <sup>14</sup>N nucleus) and drop the nuclear spin index  $i$ . To describe the NV-nucleus flip-flop, we decompose the HFI into the longitudinal part  $\hat{F}_z \hat{I}_z$  that conserves the nuclear spin and the transverse part  $(\hat{F}_+ \hat{I}_- + h.c.)/2$  that induces NV-nucleus spin flip-flop dynamics. As we always work near the GSLAC, the nuclear spin flip induced by the off-resonant excited state HFI is very small (to be discussed shortly). Since  $|-1_g\rangle$  is nearly degenerate with the NV steady state  $|0_g\rangle$  under optical pumping, the NV-nucleus flip-flop is dominated by the  $\hat{\sigma}_{-1_g,0_g} \hat{I}_+$  pro-

cess  $|0_g\rangle \otimes |m\rangle \rightarrow |-1_g\rangle \otimes |m+1\rangle$  and the  $\hat{\sigma}_{-1_g,0_g} \hat{I}_-$  process  $|0_g\rangle \otimes |m+1\rangle \rightarrow |-1_g\rangle \otimes |m\rangle$ , where  $\{|m\rangle\}$  are nuclear spin Zeeman eigenstates. The corresponding energy mismatches of these two processes are

$$\begin{aligned} \Delta_{m+1 \leftarrow m} &\equiv \Delta + \gamma_N B - (m+1)A_{g,zz}, \\ \Delta_{m \leftarrow m+1} &\equiv \Delta - \gamma_N B - mA_{g,zz}, \end{aligned}$$

respectively, where the first term  $\Delta \equiv D_{gs} - \gamma_e B$  is the  $|-1_g\rangle$ - $|0_g\rangle$  energy separation, the second term  $\pm \gamma_N B$  comes from the nuclear spin Zeeman term, while the last term comes from the longitudinal HFI  $\hat{F}_z \hat{I}_z \approx -(A_{g,zz} \hat{\sigma}_{-1_g,-1_g} + A_{e,zz} \hat{\sigma}_{-1_e,-1_e}) \hat{I}_z$ . The energy mismatch difference

$$\Delta_N \equiv \Delta_{m+1 \leftarrow m} - \Delta_{m \leftarrow m+1} = 2\gamma_N B - A_{g,zz} \quad (1)$$

provide the first essential ingredient for engineering the DNP by selectively driving one process into resonance.

The second essential ingredient for engineering the dissipative DNP is optical pumping, which connects the NV center to the strongly dissipative bath of vacuum electromagnetic fluctuation and makes the NV center itself a dissipative, non-equilibrium bath: it quickly establishes the unique steady state  $|0_g\rangle$  whatever the initial state is (commonly known as optical initialization). When optical pumping is not too weak, such that the NV dissipation (more precisely the NV optical initialization) is much faster than nuclear spin dissipation (more precisely the DNP process), the NV center can be regarded as always in its steady state  $|0_g\rangle$ , i.e., it becomes a Markovian bath and induces DNP by driving the two processes  $\hat{\sigma}_{-1_g,0_g} \hat{I}_\pm$ <sup>24</sup>. The resonance linewidth of both processes are determined by the optically induced NV ground state level broadening. Therefore, under sufficiently weak (but not too weak) optical pumping such that the linewidth of each resonance is much narrower than the distance  $|\Delta_N|$  between the two resonances, we can fine tune the magnetic field to drive  $\hat{\sigma}_{-1_g,0_g} \hat{I}_+$  ( $\hat{\sigma}_{-1_g,0_g} \hat{I}_-$ ) into resonance, while keeping  $\hat{\sigma}_{-1_g,0_g} \hat{I}_-$  ( $\hat{\sigma}_{-1_g,0_g} \hat{I}_+$ ) off-resonance to achieve strong positive (negative) nuclear polarization. When the magnetic field is swept from  $\hat{\sigma}_{-1_g,0_g} \hat{I}_+$  resonance to  $\hat{\sigma}_{-1_g,0_g} \hat{I}_-$  resonance, the <sup>13</sup>C nuclear polarization changes from positive values to negative values over a magnetic field range  $\sim |\Delta_N|/\gamma_e$ . For first-shell <sup>13</sup>C nuclei,  $|\Delta_N|$  is dominated by  $|A_{g,zz}| \approx 130$  MHz. This gives a simple explanation to the experimentally observed polarization sign reversal over a few mT<sup>24</sup>. For weakly coupled <sup>13</sup>C nuclei,  $|\Delta_N| \approx 2|\gamma_N B| \approx 2.2$  MHz is greatly reduced, corresponding to a much more sensitive dependence of the <sup>13</sup>C polarization on the magnetic field over a range  $\sim 0.1$  mT. Below we demonstrate this intuitive idea and provide a complete picture for the DNP of a single nuclear spin- $I$  before going into the more complicated case of multi-nuclei DNP.

### DNP theory of single nuclear spin

Under optical pumping from the NV ground orbital  $|g\rangle$  to the excited orbital  $|e\rangle$ , seven NV states are relevant, including the ground state triplet, excited state triplet, and a

metastable singlet state  $|S\rangle$  [see Fig. 1(a)]. The NV Hamiltonian consists of the orbital part  $\omega_0\hat{\sigma}_{e,e}$ , the optical pumping term  $\hat{H}_e(t) = (\Omega_R/2)e^{-i\omega t}\hat{\sigma}_{e,g} + h.c.$ , the ground state triplet part  $\hat{H}_{gs} \equiv D_{gs}\hat{S}_{g,z}^2 + \gamma_e B\hat{S}_{g,z}$ , and the excited state triplet part  $\hat{H}_{es} \equiv D_{es}\hat{S}_{e,z}^2 + \gamma_e B\hat{S}_{e,z}$ , where  $\hat{\sigma}_{i,j} \equiv |i\rangle\langle j|$  is the transition operator. In the rotating frame of the optical pumping, the NV-nucleus coupled system obeys

$$\dot{\hat{\rho}}(t) = \mathcal{L}_{\text{NV}}\hat{\rho}(t) - i[\hat{H}_N + \hat{\mathbf{F}} \cdot \hat{\mathbf{I}}, \hat{\rho}(t)], \quad (2)$$

where  $\hat{H}_N = \gamma_N B\hat{I}_z$  is the nuclear spin Zeeman Hamiltonian and  $\mathcal{L}_{\text{NV}}(\cdot) \equiv -i[\hat{H}_{\text{NV}}, (\cdot)] + \sum_{\alpha} \mathcal{D}[\hat{L}_{\alpha}](\cdot)$  is the evolution superoperator of the NV center in the absence of the nuclear spin, with  $\hat{H}_{\text{NV}}$  the NV Hamiltonian in the rotating frame and the last term accounting for various NV dissipation channels [shown in Fig. 1(a)] in the Lindblad form  $\mathcal{D}[\hat{L}]\hat{\rho} \equiv (\hat{L}\hat{\rho}\hat{L}^\dagger - \{\hat{L}^\dagger\hat{L}, \hat{\rho}\}/2)$ , as well as the excited orbital pure dephasing at a rate  $\Gamma_e$  and the ground state spin dephasing at a rate  $\gamma_\varphi = 1/T_{2,\text{NV}}$  that models the finite ground state coherence time  $T_{2,\text{NV}}$ . We use the experimentally measured dissipation rates at room temperature:  $\Gamma_e = 10^4$  GHz<sup>38</sup>,  $\gamma = 13$  MHz<sup>39</sup>,  $\gamma_1 \approx 13.3$  MHz<sup>40</sup>, and  $\gamma_s = 0.56$  MHz<sup>41-44</sup>. Here we have neglected the very small leakage via intersystem crossing from  $|0_e\rangle$  to  $|\pm 1_g\rangle$ , consistent with the experimentally reported<sup>14,45</sup> high optical initialization probability  $\sim 96\%$  into  $|0_g\rangle$ . Indeed, we have verified that the nuclear polarization is not so sensitive to the optical initialization probability, e.g., upon including appreciable leakage such that the optical initialization probability drops to 80%, the steady-state <sup>13</sup>C nuclear polarization drops by  $\sim 20\%$ .

The DNP can be directly obtained by solving Eq. (2) numerically. However, this approach does not provide a clear physics picture for the underlying DNP mechanism and is not suitable for searching for optimal experimental parameters to maximize the DNP effect. Further, for the DNP of multiple nuclear spins (to be discussed shortly), this approach quickly becomes infeasible with increasing number  $N$  of the nuclei, because the dimension of the Liouville space grows exponentially as  $\dim(\hat{\rho}) \approx (2I + 1)^{2N} M^2$ , where  $M = 7$  is the number of relevant energy levels of the NV center, e.g., the DNP of  $N = 5$  nuclear spin-1/2's already involves  $\dim(\hat{\rho}) \approx 50000$  and hence is computationally intensive.

Our work is based on a recently developed microscopic theory<sup>46-48</sup>, applicable as long as the NV dissipation (optical initialization in the present case) is much faster than the nuclear spin dissipation (DNP in the present case). The populations  $\{p_m\}$  of a single nuclear spin- $I$  on its Zeeman sublevels  $|m\rangle$  ( $m = -I, -I + 1, \dots, I$ ) obey the rate equations

$$\dot{p}_m = \sum_{n=m\pm 1} W_{m\leftarrow n} p_n - \left( \sum_{n=m\pm 1} W_{n\leftarrow m} \right) p_m. \quad (3)$$

Up to second order of the *transverse* HFI (longitudinal HFI treated *exactly*), the transition rate from  $|m\rangle$  to  $|m \pm 1\rangle$  is<sup>48</sup>

$$W_{m\pm 1\leftarrow m} = \frac{\xi_m^\pm}{2} \text{Re} \int_0^{+\infty} dt e^{\mp i\gamma_N B t} \text{Tr}_{\text{NV}} \hat{F}_\mp^\dagger e^{\mathcal{L}_{m\pm 1, m} t} \hat{F}_\mp \hat{P}_m, \quad (4)$$

where  $\xi_m^\pm \equiv \langle m | \hat{I}_\mp \hat{I}_\pm | m \rangle$ , the Liouville superoperator  $\mathcal{L}_{n,m}(\bullet) \equiv \mathcal{L}_{\text{NV}}(\bullet) - i[n\hat{F}_z(\bullet) - (\bullet)m\hat{F}_z]$ , and  $\hat{P}_m$  is the NV steady state in

the rotating frame conditioned on the nuclear spin state being  $|m\rangle$ , i.e.,  $\mathcal{L}_{m,m}\hat{P}_m = 0$  and  $\text{Tr}_{\text{NV}}\hat{P}_m = 1$ . The nuclear spin depolarization by other mechanisms such as spin-lattice relaxation can be described by a phenomenological depolarization rate  $\gamma_{\text{dep}}$  and incorporated by replacing  $W_{m\pm 1\leftarrow m}$  with  $W_{m\pm 1\leftarrow m} + \xi_m^\pm \gamma_{\text{dep}}$ .

Equation (4) can be understood as a generalized fluctuation-dissipation relation<sup>49</sup>. Since the nuclear spin transition from  $|m\rangle$  to  $|m+1\rangle$  ( $|m-1\rangle$ ) is induced by the HFI term  $\hat{F}_- \hat{I}_+$  ( $\hat{F}_+ \hat{I}_-$ ) and involves the transfer of energy  $\gamma_N B$  from the NV center (nuclear spin) to the nuclear spin (NV center), the corresponding transition rate is proportional to the fluctuation of the Knight field  $\hat{F}_-$  ( $\hat{F}_+$ ) at frequency  $-\gamma_N B$  ( $+\gamma_N B$ ) in the NV steady state  $\hat{P}_m$ . Without the longitudinal HFI  $\hat{F}_z \hat{I}_z$ , we have  $\mathcal{L}_{n,m} = \mathcal{L}_{\text{NV}}$ , so  $\hat{P}_m = \hat{P}$  is the steady NV state in the absence of the nuclei, and Eq. (4) reduces to the conventional Born-Markovian approximation. As discussed above and further elaborated below, the longitudinal HFI  $\hat{F}_z \hat{I}_z$  could significantly modify the energy cost of the nuclear spin flip and hence the steady-state nuclear polarization.

In general, the nuclear spin transition rates  $W_{m\pm 1\leftarrow m}$  in Eq. (4) can be evaluated numerically (see Methods). However, the physical picture and global optimization of the experimental parameters will be greatly facilitated by explicit analytical expressions, which we present below.

### Explicit analytical expressions

Since we always consider  $B \sim 102$  mT near  $|0_g\rangle - |1_g\rangle$  GSLAC, the dominant NV-nucleus flip-flop involves the near-resonant process  $|0_g\rangle \leftrightarrow |1_g\rangle$ . This allows us to neglect  $|+1_g\rangle$  and  $|+1_e\rangle$ , describe the NV center by a five-level model [Fig. 1(b)], and derive explicit analytical expressions for the nuclear spin transition rates  $W_{m\pm 1\leftarrow m}$  (see Methods). For general parameters, the expressions are complicated due to the presence of various quantum coherence effects associated with the optical pumping induced  $|0_g\rangle - |0_e\rangle$  and  $|1_g\rangle - |1_e\rangle$  oscillation. However, if we focus on weak optical pumping far from saturation, i.e., optical pumping rate  $R \equiv \Omega_R^2/\Gamma_e \ll$  linewidth  $\gamma + \gamma_1/2 \approx 26.3$  MHz of  $|0_e\rangle \leftrightarrow |1_e\rangle$  transition, then the quantum coherence effects are negligible and  $W_{m\pm 1\leftarrow m}$  assume the appealing form of a Fermi golden rule

$$W_{m\pm 1\leftarrow m} = P_g \xi_m^\pm 2\pi \left| \frac{A_{g,+ \mp}}{2\sqrt{2}} \right|^2 \delta^{(\Gamma)}(\Delta_{m\pm 1\leftarrow m}), \quad (5)$$

where  $P_g = (R + \gamma)/(2R + \gamma)$  is the steady-state populations on  $|0_g\rangle$ ,  $\delta^{(\gamma)}(x) \equiv (\gamma/\pi)/(x^2 + \gamma^2)$  is the Lorentzian shape function,  $\Gamma \equiv \gamma_\varphi + R$  is the resonance linewidth, and  $A_{g,+ \mp} \equiv \mathbf{e}_+ \cdot \mathbf{A}_g \cdot \mathbf{e}_\mp$  ( $\mathbf{e}_\pm \equiv \mathbf{e}_x \pm i\mathbf{e}_y$ ) quantifies the coefficient of the term  $\hat{\sigma}_{-1_g, 0_g} \hat{I}_\pm$  in the transverse HFI. A key feature of Eq. (5) is that the resonance linewidth of both nuclear spin-flip processes is the sum of  $|0_g\rangle - |1_g\rangle$  decoherence rate  $\gamma_\varphi = 1/T_{2,\text{NV}}$  ( $\sim 1$  kHz  $\ll$  typically  $R$ ) and optical pumping induced NV level broadening (which equals the optical pumping rate  $R$ ). This result provides a clear understanding of the laser induced NV ground state level broadening previ-

ously observed in the cross-relaxation between the NV center and nearby nitrogen impurities<sup>23,50</sup>. Further, it indicates that under sufficiently weak pumping, the opposite processes  $W_{m+1 \leftarrow m}$  and  $W_{m \leftarrow m+1}$  can be selectively driven into resonance to achieve strong nuclear spin polarization. Equation (5) also reveals that the DNP depends strongly on the form of the HFI tensor  $\mathbf{A}_g$ , e.g., for the  $^{14}\text{N}$  or  $^{15}\text{N}$  nucleus with isotropic transverse HFI  $A_{g,xx} = A_{g,yy}$  and  $A_{g,xy} = 0$ , we have  $A_{g,++} = 0$  and  $A_{g,+ -} = 2A_{g,xx}$  and hence complete positive polarization.

Equation (5) can be applied to a general nuclear spin- $I$ , but hereafter we focus on a  $^{13}\text{C}$  nuclear spin-1/2 and define  $W_+ \equiv W_{\uparrow \leftarrow \downarrow}$  and  $W_- \equiv W_{\downarrow \leftarrow \uparrow}$ , given by Eq. (5) as

$$W_{\pm} = P_g 2\pi \left| \frac{A_{g,+ \mp}}{2\sqrt{2}} \right|^2 \delta^{(I)}(\Delta \pm \Delta_N/2). \quad (6)$$

The evolution of the nuclear polarization  $p \equiv 2\langle \hat{I}_z \rangle$  follows from  $\dot{p}(t) = -W[p(t) - p_{ss}]$  as  $p(t) = p_{ss} + [p(0) - p_{ss}]e^{-Wt}$ , so the DNP of a  $^{13}\text{C}$  nuclear spin is completely determined by two key quantities: the steady-state polarization  $p_{ss} \equiv (W_+ - W_-)/(W_+ + W_-)$  and the rate  $W \equiv W_+ + W_-$  of DNP. Up to now, we have neglected other nuclear spin relaxation mechanisms, such as spin-lattice relaxation and transverse HFI with NV excited states. The former occurs on the time scale ranging from a few seconds to tens of minutes<sup>17,51</sup>. The latter occurs on the time scale  $1/W_{es}$ , where  $W_{es}$  can be estimated from the Fermi golden rule as  $2\pi(A_e/2)^2 \delta^{(\gamma+\gamma_1/2)}(D_{es})P_e$ , e.g., for a  $^{13}\text{C}$  located at  $|\mathbf{R}| > 3 \text{ \AA}$  coupled to the NV excited states via dipolar HFI, we have  $1/W_{es} > 1 \text{ s}$  for  $R = 0.2 \text{ MHz}$ . These effects are described by nuclear depolarization  $W_{\pm} \rightarrow W_{\pm} + \gamma_{dep}$ , which increases  $W$  by  $2\gamma_{dep}$  and decreases  $p_{ss}$  by a factor  $1 + 2\gamma_{dep}/W$ , i.e., nuclear depolarization is negligible when  $W \gg 2\gamma_{dep}$ .

Finally we emphasize that our rate equation theory and hence Eq. (6) are accurate when the DNP time  $1/W$  from Eq. (6)  $\gg$  NV optical initialization time  $\tau_c \approx ([R\gamma_1/(\gamma_1 + \gamma)]^{-1} + \gamma_s^{-1})$ . When the optical pumping is so weak that the calculated DNP time from Eq. (6) drops below  $\tau_c$ , the NV center becomes a non-Markovian bath and the true DNP time would be lower bounded by  $\sim \tau_c$ , as we discuss below.

### DNP of strongly coupled $^{13}\text{C}$ nucleus

To begin with, we consider the DNP of a strongly coupled  $^{13}\text{C}$  nucleus in the first shell of the NV center under optical pumping near the  $|0_g\rangle - |1_g\rangle$  GSLAC. This configuration has been studied experimentally in ensembles of NV centers<sup>24</sup>, which reveals an interesting polarization sign reversal over a narrow range of magnetic fields. This is attributed to the anisotropic HFI and could allow magnetic control of the  $^{13}\text{C}$  nuclear polarization, but a quantitative understanding remains absent. Here we provide a clear physics picture and parameter-free explanation for this sign reversal using the experimentally measured ground state HFI tensor<sup>19,24,31,33</sup>  $A_{g,xx} = 198.6 \text{ MHz}$ ,  $A_{g,yy} = 123.0 \text{ MHz}$ ,  $A_{g,zz} = 129.0 \text{ MHz}$ ,  $A_{g,xz} = A_{g,zx} = -21.5 \text{ MHz}$ , and excited state HFI tensor<sup>19</sup>  $A_{e,xx} = 103.2 \text{ MHz}$ ,  $A_{e,yy} = 56.7 \text{ MHz}$ ,  $A_{e,zz} = 79.5 \text{ MHz}$ ,

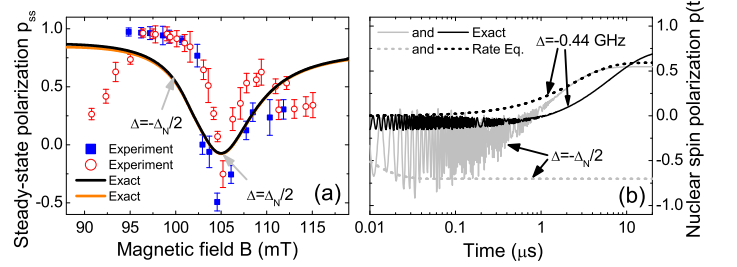


FIG. 2. (a)  $p_{ss}$  of a first-shell  $^{13}\text{C}$  nucleus: exact solution to Eq. (2) with (orange solid line) or without (black solid line) excited state HFI, compared with the experimental data<sup>24</sup> (filled squares and empty circles) from two different analysis methods. (b) Real-time evolution of nuclear polarization  $p(t)$  on  $W_+$  resonance ( $\Delta = -\Delta_N/2$ ) or far from the resonance ( $\Delta = -0.44 \text{ GHz}$ ): exact solution to Eq. (2) vs. our rate equation theory [Eqs. (3) and (4)].

$A_{e,xz} = A_{e,zx} = -32.6 \text{ MHz}$ . To focus on the intrinsic behavior of DNP induced by the ground state HFI, we set  $\gamma_{dep} = 0$ . We have verified that due to the strong HFI induced NV- $^{13}\text{C}$  mixing, the magnetic field dependence of the  $^{13}\text{C}$  nuclear polarization depends weakly on the optical pumping up to  $R < 4 \text{ MHz}$ . In our numerical calculation, we take  $R = 0.4 \text{ MHz}$ .

First we discuss the exact solution to the Lindblad master equation Eq. (2) without the excited state HFI. In Fig. 2(a), the calculated steady-state polarization  $p_{ss}$  (black solid lines) agrees reasonably with the experimental data<sup>24</sup>. According to our analytical expression Eq. (6), the negative dip at  $B \approx 105 \text{ mT}$  and positive shoulder at  $B \approx 100 \text{ mT}$  correspond, respectively, to  $W_-$  resonance at  $\Delta = \Delta_N/2$  and  $W_+$  resonance at  $\Delta = -\Delta_N/2$ . The strong transverse HFI leads to rapid DNP and significant non-Markovian oscillation in the real-time evolution of the nuclear polarization  $p(t)$  [solid lines in Fig. 2(b)], beyond the description of our rate equation theory. Going successively closer to GSLAC, the DNP time shortens [Fig. 2(b)] and finally saturates at  $\sim 1.6 \mu\text{s}$ , lower bounded by the NV optical initialization time  $\tau_c \approx 1.1 \mu\text{s}$ . The small difference between the black and orange solid lines in Fig. 2(a) confirms that the far off-resonant excited state HFI has a negligible effect. Indeed, the exact numerical solution to Eq. (2) including the excited state HFI shows that over the whole range of magnetic field under consideration, the excited state HFI alone polarizes the nuclear spin towards  $p_{ss} \sim 0.5$  with a DNP time  $\sim 30\text{-}40 \mu\text{s}$  (much slower than the ground state HFI induced DNP), consistent with the estimation based on the Fermi golden rule.

Next we demonstrate that our analytical expression Eq. (6) is accurate as long as the Markovian condition  $W \ll 1/\tau_c$  is satisfied, e.g., for magnetic field away from GSLAC or for  $^{13}\text{C}$  nuclei with weaker transverse HFI. For this purpose, we manually scale down  $A_{g,xx}$  and  $A_{g,yy}$  by a factor  $\eta$  to decrease the DNP rate, but keep the longitudinal component  $A_{g,zz}$  invariant. In Fig. 3(a), the analytical nuclear polarization  $p_{ss}$  agrees well with the exact solution to Eq. (2) for  $\eta \gtrsim 5$ . In Fig. 3(b), when approaching  $W_{\pm}$  resonances, the analytical DNP rate from Eq. (6) sharply peaks and significantly exceeds  $1/\tau_c \approx (1.1 \mu\text{s})^{-1}$ , while the exact solution saturates to  $\sim (1.6 \mu\text{s})^{-1}$ . Away from

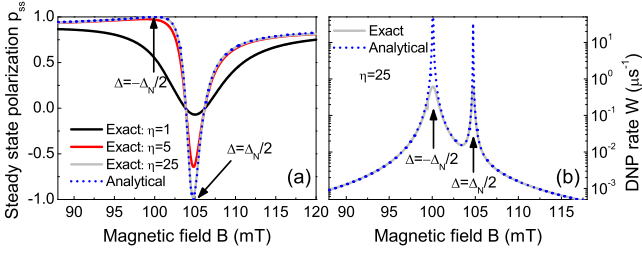


FIG. 3. (a) Steady-state polarization  $p_{ss}$  of a first-shell  $^{13}\text{C}$  nucleus: exact numerical solution to Eq. (2) (solid lines) vs. analytical formula Eq. (6) (dotted line). To illustrate the convergence of our theory, we scale down the transverse HFI ( $A_{g,xx}$  and  $A_{g,yy}$ ) by a factor  $\eta = 1$  (black line), 5 (red line), and 25 (gray line), with  $A_{g,xz} = A_{g,zx} = 0$  for  $\eta = 5$  and 25 to avoid spurious behaviors. (b) DNP rate for  $\eta = 25$ : exact solution to Eq. (2) (gray solid line) vs. analytical formula Eq. (6) (blue dotted line).

$W_{\pm}$  resonances, our analytical DNP rate  $\ll 1/\tau_c$  and hence agrees well with the exact solution.

In the above, for a first-shell  $^{13}\text{C}$  nuclear spin, the separation  $\Delta_N = 2\gamma_N B - A_{g,zz} \approx -131$  MHz is dominated by the strong HFI term. Consequently, the magnetic fields for the two resonances at  $\Delta = \pm\Delta_N/2$  are separated by  $\Delta_N/(\gamma_e B) \approx 5$  mT, which determines the magnetic field sensitivity of the polarization sign reversal in Fig. 3(a). This suggests that for weakly coupled  $^{13}\text{C}$  nuclear spins with much smaller  $\Delta_N \approx -2$  MHz, the magnetic field sensitivity can be greatly enhanced.

### DNP of weak coupled $^{13}\text{C}$ nucleus

Now based on the analytical expression Eq. (6), we provide a complete picture for the dependence of the DNP rate  $W$  and steady-state polarization  $p_{ss}$  on the resonance linewidth  $\Gamma \approx R$ , the  $|0_g\rangle - |1_g\rangle$  separation  $\Delta = D_{gs} - \gamma_e B$ , and the hyperfine tensor  $\mathbf{A}_g$ . It reveals the possibility to strongly polarize a weakly coupled, distant  $^{13}\text{C}$  nucleus.

The simplest case is strong optical pumping with the resonance linewidth  $\Gamma > |\Delta_N|$ , i.e., the  $W_{\pm}$  resonance peaks at  $\Delta = -\Delta_N/2$  and  $\Delta = \Delta_N/2$ , respectively, are not spectrally resolved:  $W_{\pm} \approx \pi(|A_{g,+}|^2/4)\delta^{(\Gamma)}(\Delta)$ . In this case  $p_{ss}$  is uniquely determined by the HFI tensor  $\mathbf{A}_g$ , but  $W$  still depends on the  $|0_g\rangle - |1_g\rangle$  separation  $\Delta$  and becomes suppressed when  $|\Delta| \gg \Gamma$ . For dipolar HFI,

$$\begin{aligned} A_{g,zz} &= -A_{g,+} = A_{dp}(|\mathbf{R}|)(1 + c_{\theta}), \\ A_{g,++} &= A_{dp}(|\mathbf{R}|)(1 - c_{\theta})e^{2i\varphi}, \end{aligned}$$

where  $A_{dp}(|\mathbf{R}|) \equiv -\mu_0\gamma_e\gamma_N/(4\pi|\mathbf{R}|^3) \approx 20$  MHz  $\text{\AA}^3/|\mathbf{R}|^3$ ,  $\gamma_N = -10.705$  MHz/T is the  $^{13}\text{C}$  nuclear gyromagnetic ratio,  $c_{\theta} \equiv 3\cos^2\theta - 2$ , and  $\theta$  ( $\varphi$ ) is the polar (azimuth) angle of the  $^{13}\text{C}$  location  $\mathbf{R}$ . Thus the polarization

$$p_{ss} \approx \frac{2}{c_{\theta} + 1/c_{\theta}} \quad (7)$$

is uniquely determined by the polar angle  $\theta$  and is independent

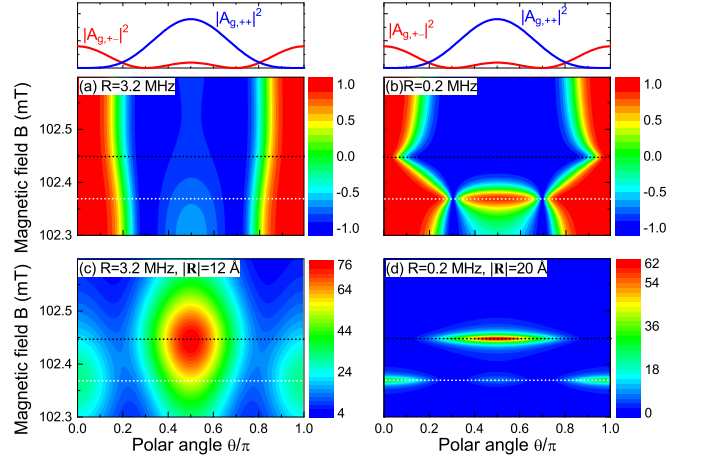


FIG. 4. Steady state nuclear polarization  $p_{ss}$  [(a) and (b)] and DNP rate  $W$  in units of Hz [(c) and (d)] by dipolar HFI with the NV center, calculated from the analytical formula Eq. (6) with optical pumping rates  $R = 3.2$  MHz [(a) and (c)] and 0.2 MHz [(b) and (d)]. The distance of the  $^{13}\text{C}$  nucleus from the NV center is  $|\mathbf{R}| = 12$   $\text{\AA}$  in (c) and  $|\mathbf{R}| = 20$   $\text{\AA}$  in (d). The white (black) dotted line indicates the critical magnetic field for  $W_+$  ( $W_-$ ) resonance.

of  $|\mathbf{R}|$  as long as the DNP rate  $W \gg 2\gamma_{dp}$  or equivalently

$$A_{dp}^2(|\mathbf{R}|) \gg 4\Gamma\gamma_{dp}, \quad (8)$$

e.g., for  $\Gamma = 0.2$  MHz and  $\gamma_{dp} = 1$  s $^{-1}$ , this condition amounts to  $A_{dp} > 1$  kHz and is satisfied by nuclei with  $|\mathbf{R}| < 27$   $\text{\AA}$ . An example for strong optical pumping is shown in Figs. 4(a) and 4(c). In Fig. 4(c), the  $W_+$  resonance peak (marked by white dotted lines) and the  $W_-$  resonance peak (marked by black dotted lines) are significantly broadened along the magnetic field axis and are not clearly resolved. Consequently, the nuclear polarization in Fig. 4(a) follows the HFI coefficients  $|A_{g,+}|^2 \propto (1 \pm c_{\theta})^2$  [plotted on top of Figs. 4(a) and 4(b)] and is well described by Eq. (7).

The most interesting case is weak optical pumping with the resonance linewidth  $\Gamma \ll |\Delta_N|$ . In this case, the  $W_{\pm}$  resonance peaks are spectrally resolved and can be selectively driven into resonance to achieve strong nuclear polarization  $p_{ss} = \pm\Delta_N^2/(\Delta_N^2 + 2\Gamma^2) \approx \pm 100\%$  by choosing  $\Delta = \mp\Delta_N/2$ . The DNP rate  $W \propto 1/\Gamma$  is dominated by the resonant process and can be increased up to the saturation value  $\sim 1/\tau_c$  by decreasing the linewidth  $\Gamma$ . An example is given in Figs. 4(b) and 4(d). In Fig. 4(d), the very narrow  $W_+$  resonance peak at  $\Delta = -\Delta_N/2$  (corresponding to  $B \approx 102.37$  mT, marked by white dotted lines) and the  $W_-$  resonance peak at  $\Delta \approx \Delta_N/2$  (corresponding to  $B \approx 102.45$  mT, marked by black dotted lines) can be clearly resolved. In Fig. 4(b), the  $W_{\pm}$  resonances give rise to fine structures in the nuclear polarization  $p_{ss}$  near  $B \approx 102.37$  mT and  $B \approx 102.45$  mT, superimposed on the usual dependence on the polar angle  $\theta$  via  $W_{\pm} \propto |A_{g,+}|^2 \propto (1 \pm c_{\theta})^2$  [plotted on top of Figs. 4(a) and 4(b)]. We notice that a  $^{13}\text{C}$  nucleus located at  $|\mathbf{R}| = 20$   $\text{\AA}$  away from the NV center can be highly polarized with a DNP rate  $\sim 60$  Hz =  $(2.6$  ms) $^{-1}$ , sufficient to overcome the slow

nuclear depolarization  $\gamma_{\text{dep}} \sim 1 \text{ s}^{-1}$ .

Finally we present the three conditions for achieving strong nuclear polarization:

1. The linewidth  $\Gamma \ll |\Delta_N| = |2\gamma_N B - A_{g,zz}|$ , where  $2\gamma_N B \approx -2.2 \text{ MHz}$  since we always consider  $B \sim 102 \text{ mT}$  near the GSLAC. Therefore,  $|\Delta_N|$  ranges from  $\sim 2 \text{ MHz}$  (dominated by  $2\gamma_N B$ ) for weakly coupled nuclei to  $\sim 100 \text{ MHz}$  (dominated by  $A_{g,zz}$ ) for strongly coupled nuclei.
2. For optimal performance, the  $|-1_g\rangle$ - $|0_g\rangle$  separation  $\Delta$  should be tuned accurately to match one resonance peak. This requires the mismatch  $\delta\Delta < \Gamma, |\Delta_N|$ , i.e., the magnetic field control precision  $\delta B$  should be smaller than  $|\Delta_N|/\gamma_e$  ( $\sim 0.8 \text{ G}$  for weakly coupled nuclei with  $|\Delta_N| \approx 2.2 \text{ MHz}$  near GSLAC) and  $\Gamma/\gamma_e$  ( $\sim 0.07 \text{ G}$  for  $\Gamma = 0.2 \text{ MHz}$ ), accessible by current experimental techniques, e.g.,  $\delta B = 0.02 \text{ G}$  has been reported<sup>51</sup>. If the control precision  $\delta\Delta \gg$  linewidth  $\Gamma$ , then the DNP rate would be reduced by a factor  $(\delta\Delta/\Gamma)^2$ . Taking 4(d) as an example, a large magnetic field control error  $\delta B = 1 \text{ G}$  and hence  $\delta\Delta = 2.8 \text{ MHz}$  would reduce the maximal DNP rate from  $\sim 60 \text{ Hz}$  to  $\sim 2 \text{ s}^{-1}$ , which is still comparable with the depolarization rate  $\gamma_{\text{dep}} \sim 1 \text{ s}^{-1}$ .
3. For DNP to dominate over nuclear depolarization, the transverse HFI strength should satisfy

$$|A_{g,++}|^2 + |A_{g,+}|^2 \gg 4\Gamma\gamma_{\text{dep}},$$

which reduces to Eq. (8) for dipolar HFI.

### DNP of multiple $^{13}\text{C}$ nuclei

Having established a completely picture for single- $^{13}\text{C}$  DNP, now we generalize the above results to many ( $N \gg 1$ )  $^{13}\text{C}$  nuclear spins coupled to the NV center via  $\hat{H}_{\text{HF}} = \sum_{i=1}^N \hat{\mathbf{F}}_i \cdot \hat{\mathbf{I}}_i$ , where  $\hat{\mathbf{F}}_i = \hat{\mathbf{S}}_g \cdot \mathbf{A}_i$  and the excited state HFI is neglected because the induced NV-nuclei flip-flop processes are off-resonant. In the same spirit as that in treating the DNP of a single nuclear spin, we decompose the HFI into the longitudinal part  $\sum_{i=1}^N \hat{F}_{i,z} \hat{I}_{i,z}$  and the transverse part  $\sum_{i=1}^N (\hat{F}_{i,+} \hat{I}_{i,+} + h.c.)/2$ . Then we approximate the longitudinal HFI with  $-\hat{\sigma}_{-1_g, -1_g} \hat{h}_z$  (which is treated *exactly*) and treat the transverse HFI with second-order perturbation theory, where

$$\hat{h}_z \equiv \sum_{i=1}^N A_{i,zz} \hat{I}_{i,z}$$

is the collective Overhauser field from all the nuclei.

The physics picture of the many-nuclei DNP is as follows. Up to leading order, the flip of different nuclei by the transverse HFI is independent, in the sense that at a given moment, only one nuclear spin is being flipped, while other nuclear spins simply act as ‘‘spectators’’. However, the flip of each individual nuclear spin does depend on the states of all the nuclear spins via the collective Overhauser field  $\hat{h}_z$ : each many-nuclei state  $|\mathbf{m}\rangle = \otimes_{i=1}^N |m_i\rangle$  ( $|m_i\rangle$  is the Zeeman eigenstate of the  $i$ th nucleus) produces an Overhauser field

$h_{\mathbf{m}} \equiv \langle \mathbf{m} | \hat{h}_z | \mathbf{m} \rangle$  that shifts the energy of the NV state  $|-1_g\rangle$  by an amount  $-h_{\mathbf{m}}$ . This renormalizes the  $|-1_g\rangle$ - $|0_g\rangle$  separation from  $\Delta = D_{gs} - \gamma_e B$  to  $\Delta - h_{\mathbf{m}}$  and hence changes the NV dynamics and NV-induced nuclear spin flip, e.g., the spin flip rate  $W_{i,\pm}(h_{\mathbf{m}})$  of the  $i$ th nucleus conditioned on the many-nuclei state being  $|\mathbf{m}\rangle$  is obtained from Eq. (6) by replacing  $\mathbf{A}_g, \Delta$  with  $\mathbf{A}_i, \Delta - h_{\mathbf{m}}$ , respectively.

The above physics picture is quantified by the following rate equations for the diagonal elements  $p_{\mathbf{m}} \equiv \langle \mathbf{m} | \hat{\rho} | \mathbf{m} \rangle$  of the many-nuclei density matrix  $\hat{\rho}$ :

$$\begin{aligned} \dot{p}_{\mathbf{m}} = & - \sum_i [W_{i,+}(h_{\mathbf{m}}) p_{\mathbf{m}} - W_{i,-}(h_{\mathbf{m}+1_i}) p_{\mathbf{m}+1_i}] \\ & - \sum_i [W_{i,-}(h_{\mathbf{m}}) p_{\mathbf{m}} - W_{i,+}(h_{\mathbf{m}-1_i}) p_{\mathbf{m}-1_i}], \end{aligned} \quad (9)$$

which has been derived by adiabatically decoupling the fast electron dynamics from the slow DNP process<sup>46-48</sup>. Here  $|\mathbf{m}+1_i\rangle = \hat{I}_i^+ |\mathbf{m}\rangle / \sqrt{\xi_{m_i}^+}$  is the same as  $|\mathbf{m}\rangle$  except that the state of the  $i$ th nucleus changes from  $|m_i\rangle$  to  $|m_i+1\rangle$ . Now we discuss the difference between single-spin DNP and many-spin DNP. In the latter case, the DNP of each individual nucleus occurs in the presence of many ‘‘spectator’’ nuclei, which produce a fluctuating Overhauser field  $\hat{h}_z$  that randomly shifts the NV energy levels, such that the  $|-1_g\rangle$ - $|0_g\rangle$  separation changes from  $\Delta$  to a random value  $\Delta - \hat{h}_z$ . This makes it more difficult to tune the magnetic field to match the  $W_+$  (or  $W_-$ ) resonance exactly. More precisely, a finite mismatch  $\sim (h_z)_{\text{rms}}$  makes the originally resonant  $W_+$  ( $W_-$ ) process off-resonant, and hence reduce the resonant DNP rate by a factor  $(h_z)_{\text{rms}}^2/\Gamma^2$ . For example, a natural abundance of  $^{13}\text{C}$  nuclei gives a typical Overhauser field  $(h_z)_{\text{rms}} \sim 0.2 \text{ MHz}$ . This reduces the typical DNP rate by a factor of 2 for the linewidth  $\Gamma \approx R = 0.2 \text{ MHz}$ , e.g., the maximal DNP rate  $\sim 60 \text{ Hz}$  [Fig. 4(d)] for a  $^{13}\text{C}$  nucleus at  $2 \text{ nm}$  away from the NV center is reduced to  $30 \text{ Hz} \approx (5 \text{ ms})^{-1}$ , which is still sufficient to overcome the slow nuclear depolarization  $\gamma_{\text{dep}} \sim 1 \text{ s}^{-1}$ . Therefore, under weak pumping  $\Gamma \ll |\Delta_N|$ , the typical Overhauser field fluctuation  $(h_z)_{\text{rms}} \ll |\Delta_N|$  does not significantly influence the steady state nuclear polarization.

For  $N$  nuclear spin-1/2's, the number of variables  $\{p_{\mathbf{m}}\}$  is  $2^N$ . When  $N$  is small, we can solve Eq. (9) exactly. For large  $N$ , however, the exponentially growing complexity prohibit an exact solution to Eq. (9). Here, we introduce an approximate solution. The essential idea is to assume small inter-spin correlation, so that the  $N$ -nuclei density matrix  $\hat{\rho}$  can be factorized as  $\hat{\rho} = \otimes_{i=1}^N \hat{\rho}_i$ , where the  $i$ th nuclear spin state  $\hat{\rho}_i \approx |\uparrow_i\rangle\langle\uparrow_i| (1+p_i)/2 + |\downarrow_i\rangle\langle\downarrow_i| (1-p_i)/2$  is described by its polarization  $p_i$ . This dramatically reduces the number of variables from  $2^N$  many-nuclei populations  $\{p_{\mathbf{m}}\}$  to  $N$  single-spin polarizations  $\{p_i\}$ . Substituting this approximation into Eq. (9) and tracing over all the nuclei except for the  $i$ th nucleus give  $N$  coupled equations:

$$\dot{p}_i = -(\bar{W}_{i,+} + \bar{W}_{i,-}) \left( p_i - \frac{\bar{W}_{i,+} - \bar{W}_{i,-}}{\bar{W}_{i,+} + \bar{W}_{i,-}} \right), \quad (10)$$

where  $\bar{W}_{i,\pm}$  is the spin flip rate of the  $i$ th nucleus averaged over

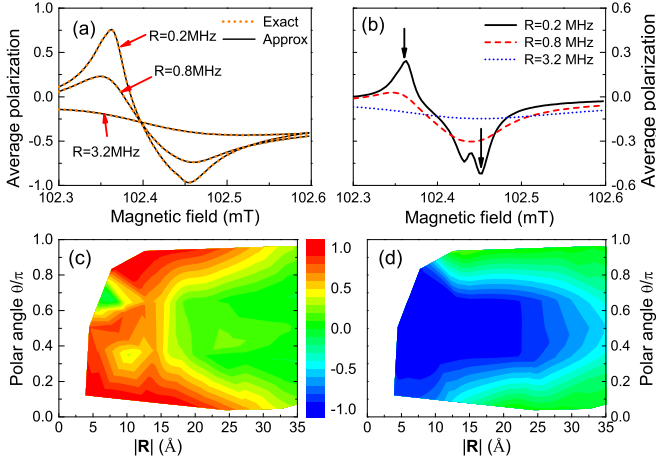


FIG. 5. Average polarization  $\bar{p}_{ss}$  of (a)  $N = 7$  and (b)  $N = 400$  randomly chosen  $^{13}\text{C}$  nuclei for different optical pumping rates  $R = 0.2, 0.8,$  and  $3.2$  MHz. For  $R = 0.2$  MHz, the spatial distribution of the polarization of  $N = 400$  randomly chosen  $^{13}\text{C}$  nuclei in a magnetic field (c)  $102.36$  mT and (d)  $102.45$  mT [marked by the arrows in panel (b)]. The depolarization rate  $\gamma_{\text{dep}} = 1$  Hz for all panels.

the states of all the other  $(N - 1)$  nuclear spins:

$$\begin{aligned}\bar{W}_{i,+} &= \text{Tr} W_{i,+}(\hat{h}_z) |\downarrow_i\rangle\langle\downarrow_i| \otimes_{j(\neq i)} \hat{p}_j, \\ \bar{W}_{i,-} &= \text{Tr} W_{i,-}(\hat{h}_z) |\uparrow_i\rangle\langle\uparrow_i| \otimes_{j(\neq i)} \hat{p}_j,\end{aligned}$$

i.e.,  $\bar{W}_{i,\pm}$  depends on the polarizations  $\{p_j\}$  ( $j \neq i$ ) of all the other nuclear spins. Therefore, Eq. (10) with  $i = 1, 2, \dots, N$  form  $N$  coupled differential equations for  $\{p_i\}$ . The steady-state solutions  $\{p_{i,ss}\}$  are obtained by solving  $N$  coupled nonlinear equations with recursive methods. This approach provides a good approximation to the average polarization  $\bar{p}_{ss} = (1/N) \sum_{i=1}^N p_{i,ss}$  and average Overhauser field  $h_{ss} = \sum_i A_{i,zz} p_{i,ss} / 2$ , but does not include any spin-spin correlation effect, such as feedback induced spin bath narrowing<sup>12,46–48,52–55</sup>.

As shown in Fig. 5(a), for a small number ( $N = 7$ ) of randomly chosen  $^{13}\text{C}$  nuclei coupled to the NV via dipolar HFI, the average polarization  $\bar{p}_{ss}$  from the above approximation agrees well with the exact solution to the rate equations. For  $N = 400$  randomly chosen  $^{13}\text{C}$  nuclei, the exact solution is no longer available and we plot the approximation results in Fig. 5(b). In both Figs. 5(a) and 5(b), we can clearly see that increasing the optical pumping strength significantly decreases the average nuclear polarization and its magnetic field dependence due to the broadening of  $W_{\pm}$  resonances. For weak optical pumping  $R = 0.2$  MHz, the average polarization  $\bar{p}_{ss}$  of 400  $^{13}\text{C}$  nuclei shows a positive maximum  $\sim +25\%$  at  $B \approx 102.36$  mT (due to  $W_+$  resonance) and a negative maximum  $\sim -55\%$  at  $B \approx 102.45$  mT (due to  $W_-$  resonance). The stronger polarization along  $-z$  axis arises from the dependence of the single-spin flip rate  $W_{\pm} \propto |A_{g,\pm}|^2 \propto (1 \pm c\theta)^2$  on the polar angle  $\theta$  of the nuclear spin location: more nuclear spins have  $|A_{g,++}|^2 > |A_{g,+}|^2$  [as plotted on top of Figs. 4(a) and 4(b)] and hence favors negative polarization. These results

clearly demonstrate the possibility to strongly polarize weakly coupled  $^{13}\text{C}$  nuclear spins by using weak optical pumping near  $W_+$  resonance ( $B \approx 102.36$  mT) or  $W_-$  resonance ( $B \approx 102.45$  mT). The steady state polarization of these weakly coupled  $^{13}\text{C}$  nuclei is ultimately limited by nuclear spin depolarization. This can be clearly seen in the spatial distribution of the nuclear polarization at the  $W_+$  resonance [Fig. 4(c)] and the  $W_-$  resonance [Fig. 4(d)]. At  $W_+$  resonance, strong positive polarization is achieved for  $^{13}\text{C}$  nuclei with  $|\mathbf{R}| < 15$  Å away from the NV center, corresponding to dipolar HFI strength  $> 6$  kHz. For more distant  $^{13}\text{C}$  nuclei, the HFI strength is too weak for the DNP to dominate over the nuclear depolarization, so their polarization drops significantly. Similarly, at  $W_-$  resonance, strong negative polarization can be achieved for  $^{13}\text{C}$  nuclei with  $|\mathbf{R}| < 25$  Å away from the NV center, corresponding to dipolar HFI strength  $\sim 1$  kHz. In principle, further decrease of the optical pumping rate  $R$  and hence the resonance linewidth  $\Gamma$  could make the  $W_{\pm}$  resonances even sharper, which allows more distant  $^{13}\text{C}$  nuclei to be strongly polarized.

Finally, we recall that the on-site  $^{15}\text{N}$  or  $^{14}\text{N}$  nucleus has an isotropic transverse HFI and hence  $W_- = |A_{g,++}|^2 = 0$ , i.e., they could be completely polarized and thus does not significantly influence the DNP of the  $^{13}\text{C}$  nuclei, except for a shift of the  $|-1_g\rangle\langle 0_g|$  separation  $\Delta$  by  $\sim 2.2$  MHz (for  $^{14}\text{N}$ ) or  $\sim 3$  MHz (for  $^{15}\text{N}$ ), corresponding to a shift of the resonance magnetic field by  $\sim 0.78$  G (for  $^{14}\text{N}$ ) or  $\sim 1.1$  G (for  $^{15}\text{N}$ ).

## DISCUSSION

In conclusion, we have presented a comprehensive theoretical understanding on the dynamic nuclear polarization induced by an optically pumped NV center near the ground state anticrossing at ambient temperature. Our results not only provide a clear physics picture for a recently observed<sup>24</sup> magnetic field dependence of the polarization of first-shell  $^{13}\text{C}$  nuclei, but also reveals an efficient scheme to strongly polarize weakly coupled  $^{13}\text{C}$  nuclear spins  $\sim 25$  Å away from the NV center (HFI strength  $\sim 1$  kHz) by weak optical pumping and fine-tuning the magnetic field. These results provide a clear guidance for optimizing future dynamic nuclear polarization experiments. For example, this scheme could be used to polarize distant  $^{13}\text{C}$  nuclei in isotope purified diamond<sup>4</sup> to further prolong the NV coherence time.

## METHODS

### Numerical evaluation of nuclear spin transition rates

Taking  $W_{m+1 \leftarrow m}$  as an example, we need to first calculate  $\hat{P}_m$  from  $\mathcal{L}_{m,m} \hat{P}_m = 0$  and  $\text{Tr}_{\text{NV}} \hat{P}_m = 1$ , and then calculate  $(\mathcal{L}_{m+1,m} - i\gamma_N B)^{-1} \hat{F}_- \hat{P}_m$ . For this purpose, we map NV operators into vectors and Liouville superoperators into matrices by introducing the complete basis set  $\{|i\rangle\langle j|\}$ , where  $i, j = 1, 2, \dots, M$ , and  $M = 7$  is the number of NV energy levels in our model [see Fig. 1(a)]. Then the NV operator  $\hat{F}_- \hat{P}_m = \sum_{ij} v_{ij} |i\rangle\langle j|$  is mapped to a vector  $\mathbf{v}$  with

components  $v_{ij} = \langle i|\hat{F}_-\hat{P}_m|j\rangle$ , and the Liouville superoperator  $\mathcal{L}_{m\pm 1,m} - i\gamma_N B$  is mapped to a matrix  $\mathbf{S}$  via  $(\mathcal{L}_{m\pm 1,m} - i\gamma_N B)|ij\rangle = \sum_{kl} |kl\rangle S_{kl,ij}$ , where the matrix element

$$S_{kl,ij} = \langle kl|[(\mathcal{L}_{m\pm 1,m} - i\gamma_N B)|i\rangle\langle j||l\rangle.$$

Then we immediately obtain  $(\mathcal{L}_{m\pm 1,m} - i\gamma_N B)^{-1}\hat{F}_-\hat{P}_m = \sum_{ij} |ij\rangle(\mathbf{S}^{-1}\mathbf{v})_{ij}$  and hence the transition rates  $W_{m\pm 1\leftarrow m}$ .

### Explicit analytical expressions for nuclear spin transition rates

With  $|+1_g\rangle$  and  $|+1_e\rangle$  neglected, the rotating frame Hamiltonian of the five-level NV model [Fig. 1(b)] is

$$\hat{H}_{\text{NV}} = \Delta\hat{\sigma}_{-1_g,-1_g} + (D_{es} - \gamma_e B + \omega_0 - \omega)\hat{\sigma}_{-1_e,-1_e} + \frac{\Omega_R}{2}(\hat{\sigma}_{-1_e,-1_g} + h.c.).$$

Neglecting  $\hat{F}_z$ -induced NV spin mixing, the longitudinal HFI reduces to  $-(A_{g,zz}\hat{\sigma}_{-1_g,-1_g} + A_{e,zz}\hat{\sigma}_{-1_e,-1_e})\hat{I}_z$ . Neglecting the non-collinear term  $\propto \hat{S}_z\hat{I}_\pm$  (as the NV mostly stays in  $|0_g\rangle$ ) and the transverse NV excited state HFI (which is far off-resonant), the transverse HFI reduces to  $(\hat{F}_+\hat{I}_- + h.c.)/2$  with  $\hat{F}_+ = (\hat{\sigma}_{-1_g,0_g}A_{g,+} + \hat{\sigma}_{0_g,-1_g}A_{g,-})/\sqrt{2}$ . To calculate  $W_{m\pm 1\leftarrow m}$  from Eq. (4), we first determine the NV steady state as  $\hat{P}_{m,m} = P_g\hat{\sigma}_{0_g,0_g} + (1 - P_g)\hat{\sigma}_{0_e,0_e}$ , where  $R = 2\pi(\Omega_R/2)^2\delta^{(\gamma+\Gamma_e+\gamma_\varphi/2)}(\omega_0 - \omega)$  is the optical pumping rate for  $|0_g\rangle \leftrightarrow |0_e\rangle$ . Substituting into Eq. (4) gives

$$W_{m\pm 1\leftarrow m} = -\xi_m^\pm \frac{|A_{g,\mp}|^2}{4} P_g \text{Re}\rho_{-1_g,0_g}^\pm, \quad (11)$$

where  $\rho_{i,j}^{(\pm)} \equiv \langle i|\hat{\rho}^{(\pm)}|j\rangle$  is the  $(i, j)$  matrix element of the operator  $\hat{\rho}^{(\pm)} \equiv (\mathcal{L}_{m\pm 1,m} \mp \gamma_N B)^{-1}\hat{\sigma}_{-1_g,0_g}$ , which is a linear combination of  $\hat{\sigma}_{-1_g,0_g}$ ,  $\hat{\sigma}_{-1_e,0_g}$ ,  $\hat{\sigma}_{-1_g,0_e}$ , and  $\hat{\sigma}_{-1_e,0_e}$  since the superoperator  $\mathcal{L}_{m\pm 1,m}$  for the five-level NV model [Fig. 1(b)] has no coherent coupling between  $\{|0_g\rangle, |0_e\rangle\}$  and  $\{|-1_g\rangle, |-1_e\rangle\}$ .

Now we calculate  $\rho_{-1_g,0_g}^{(\pm)}$  by taking the  $\langle 0_g|\bullet|-1_g\rangle, \langle -1_e|\bullet|0_g\rangle, \langle -1_g|\bullet|0_e\rangle$  and  $\langle -1_e|\bullet|0_e\rangle$  matrix elements of

$$(\mathcal{L}_{m\pm 1,m} \mp \gamma_N B)\hat{\rho}^{(\pm)} = \hat{\sigma}_{-1_g,0_g},$$

which gives four coupled equations

$$\begin{aligned} (\Delta_{-1_g,0_g}^{(\pm)} - i\Gamma_{-1_g,0_g})\rho_{-1_g,0_g}^{(\pm)} + \frac{\Omega_R}{2}(\rho_{-1_e,0_g}^{(\pm)} - \rho_{-1_g,0_e}^{(\pm)}) &= i, \\ (\Delta_{-1_e,0_g}^{(\pm)} - i\Gamma_{-1_e,0_g})\rho_{-1_e,0_g}^{(\pm)} + \frac{\Omega_R}{2}(\rho_{-1_g,0_g}^{(\pm)} - \rho_{-1_e,0_e}^{(\pm)}) &= 0, \\ (\Delta_{-1_g,0_e}^{(\pm)} - i\Gamma_{-1_g,0_e})\rho_{-1_g,0_e}^{(\pm)} - \frac{\Omega_R}{2}(\rho_{-1_g,0_g}^{(\pm)} - \rho_{-1_e,0_e}^{(\pm)}) &= 0, \\ (\Delta_{-1_e,0_e}^{(\pm)} - i\Gamma_{-1_e,0_e})\rho_{-1_e,0_e}^{(\pm)} - \frac{\Omega_R}{2}(\rho_{-1_e,0_g}^{(\pm)} - \rho_{-1_g,0_e}^{(\pm)}) &= 0. \end{aligned}$$

Here  $\Delta_{ji}^{(\pm)}$  is the energy difference between  $|j\rangle|m\pm 1\rangle$  and  $|i\rangle|m\rangle$  ( $|i\rangle, |j\rangle$  are NV states and  $|m\rangle, |m\pm 1\rangle$  are nuclear Zeeman states), i.e.,

$$\begin{aligned} \Delta_{-1_g,0_g}^{(\pm)} &= D_{gs} - \gamma_e B \pm \gamma_N B - (m\pm 1)A_{g,zz}, \\ \Delta_{-1_e,0_e}^{(\pm)} &= D_{es} - \gamma_e B \pm \gamma_N B - (m\pm 1)A_{e,zz}, \\ \Delta_{-1_e,0_g}^{(\pm)} &= E_{-1_e,0_g}^{(\pm)} + \omega_0 - \omega, \\ \Delta_{-1_g,0_e}^{(\pm)} &= E_{-1_g,0_e}^{(\pm)} - \omega_0 + \omega, \end{aligned}$$

and  $\Gamma_{ji}$  is the linewidth of the NV transition  $|i\rangle \leftrightarrow |j\rangle$ , i.e.,  $\Gamma_{-1_g,0_g} = \gamma_\varphi$ ,  $\Gamma_{-1_e,0_e} = \gamma + \gamma_1/2$ ,  $\Gamma_{-1_e,0_g} = (\Gamma_e + \gamma + \gamma_1 + \gamma_\varphi)/2$ , and  $\Gamma_{-1_g,0_e} = (\Gamma_e + \gamma + \gamma_\varphi)/2$ . Eliminating  $\rho_{-1_e,0_g}^{(\pm)}$  and  $\rho_{-1_g,0_e}^{(\pm)}$  gives the ‘‘rate equations’’:

$$\begin{aligned} (\Delta_{-1_g,0_g}^{(\pm)} - i\Gamma_{-1_g,0_g} - \mathcal{R}^{(\pm)})\rho_{-1_g,0_g}^{(\pm)} + \mathcal{R}^{(\pm)}\rho_{-1_e,0_e}^{(\pm)} &= i, \\ (\Delta_{-1_e,0_e}^{(\pm)} - i\Gamma_{-1_e,0_e} - \mathcal{R}^{(\pm)})\rho_{-1_e,0_e}^{(\pm)} + \mathcal{R}^{(\pm)}\rho_{-1_g,0_g}^{(\pm)} &= 0, \end{aligned}$$

from which we obtain the solution

$$\rho_{-1_g,0_g}^{(\pm)} = \frac{i}{\Delta_{-1_g,0_g}^{(\pm)} - i\Gamma_{-1_g,0_g} - \mathcal{R}^{(\pm)} \left( 1 + \frac{\mathcal{R}^{(\pm)}}{\Delta_{-1_e,0_e}^{(\pm)} - i\Gamma_{-1_e,0_e} - \mathcal{R}^{(\pm)}} \right)}, \quad (12)$$

where  $\mathcal{R}^{(\pm)} = \mathcal{R}_0^{(\pm)} + \mathcal{R}_{-1}^{(\pm)}$  with  $\mathcal{R}_0^{(\pm)} \equiv (\Omega_R/2)^2/(\Delta_{-1_g,0_g}^{(\pm)} - i\Gamma_{-1_g,0_g})$  and  $\mathcal{R}_{-1}^{(\pm)} \equiv (\Omega_R/2)^2/(\Delta_{-1_e,0_g}^{(\pm)} - i\Gamma_{-1_e,0_g})$  the complex self-energy corrections to  $|0_g\rangle$  and  $|-1_g\rangle$  by the optical pumping  $|0_g\rangle \leftrightarrow |0_e\rangle$  and  $|-1_g\rangle \leftrightarrow |-1_e\rangle$ , respectively. More precisely, the optical pumping  $|0_g\rangle \leftrightarrow |0_e\rangle$  ( $|-1_g\rangle \leftrightarrow |-1_e\rangle$ ) induces an optical Stark shift  $\text{Re}\mathcal{R}_0^{(\pm)}$  ( $-\text{Re}\mathcal{R}_{-1}^{(\pm)}$ ) and an effective dissipation  $\text{Im}\mathcal{R}_0^{(\pm)}$  ( $\text{Im}\mathcal{R}_{-1}^{(\pm)}$ ) for the NV ground state  $|0_g\rangle$  ( $|-1_g\rangle$ ). Taking  $\mathcal{R}_0^{(\pm)}$  as an example, if  $|\Gamma_{-1_g,0_g}|$  is much smaller than  $|E_{-1_g,0_g}^{(\pm)}|$ , then the optical Stark shift  $\delta E_{0_g} \approx (\Omega_R/2)^2/\Delta_{-1_g,0_g}^{(\pm)}$  reduces to the conventional form of a second-order energy correction in non-degenerate perturbation theory, while the dissipation  $\text{Im}\mathcal{R}_0^{(\pm)}$  takes the semiclassical form of a Fermi golden rule. Substituting Eq. (12) into Eq. (11) immediately gives  $W_{m\pm 1\leftarrow m}$ , which assumes a tedious form as it includes various quantum coherence effects.

For simplification, we use the fact that the NV excited state dephasing  $\Gamma_e \sim 10^4$  GHz  $\gg$  other NV dissipation  $\gamma, \gamma_1, \gamma_\varphi$  and typical detuning  $|\omega_0 - \omega|$ ,  $|\Delta_{-1_g,0_g}^{(\pm)}|$ , and  $|\Delta_{-1_e,0_g}^{(\pm)}|$ , and further restrict to weak optical pumping  $R \ll \Gamma_{-1_e,0_e}$  ( $\sim 26.3$  MHz). In this case, the optical Stark shift is negligible and the optical pumping rate simplifies to  $R \approx \Omega_R^2/\Gamma_e$ , so the self-energies  $\mathcal{R}^{(\pm)} \approx iR$  only induces NV level broadening. Substituting the resulting expression  $\rho_{-1_g,0_g}^{(\pm)} \approx i/(\Delta_{-1_g,0_g}^{(\pm)} - i(\gamma_\varphi + R))$  into Eq. (11) gives Eq. (5).

\* wenyang@csrc.ac.cn

<sup>1</sup> Abragam, A. *The Principles of Nuclear Magnetism* (Oxford University Press, New York, 1961).

versity Press, New York, 1961).

<sup>2</sup> Kane, B. E. A silicon-based nuclear spin quantum computer. *Nature*

- ture **393**, 133–137 (1998).
- <sup>3</sup> Gruber, A. *et al.* Scanning confocal optical microscopy and magnetic resonance on single defect centers. *Science* **276**, 2012–2014 (1997).
  - <sup>4</sup> Balasubramanian, G. *et al.* Ultralong spin coherence time in isotopically engineered diamond. *Nat. Mater.* **8**, 383–387 (2009).
  - <sup>5</sup> He, X.-F., Manson, N. B. & Fisk, P. T. H. Paramagnetic resonance of photoexcited n-v defects in diamond. i. level anticrossing in the 3a ground state. *Phys. Rev. B* **47**, 8809–8815 (1993).
  - <sup>6</sup> Jacques, V. *et al.* Dynamic polarization of single nuclear spins by optical pumping of nitrogen-vacancy color centers in diamond at room temperature. *Phys. Rev. Lett.* **102**, 057403 (2009).
  - <sup>7</sup> Maze, J. R. *et al.* Nanoscale magnetic sensing with an individual electronic spin in diamond. *Nature* **455**, 644–647 (2008).
  - <sup>8</sup> Taylor, J. M. *et al.* High-sensitivity diamond magnetometer with nanoscale resolution. *Nat. Phys.* **4**, 810–816 (2008).
  - <sup>9</sup> Childress, L. *et al.* Coherent dynamics of coupled electron and nuclear spin qubits in diamond. *Science* **314**, 281–285 (2006).
  - <sup>10</sup> Dutt, M. V. G. *et al.* Quantum register based on individual electronic and nuclear spin qubits in diamond. *Science* **316**, 1312–1316 (2007).
  - <sup>11</sup> Neumann, P. *et al.* Single-shot readout of a single nuclear spin. *Science* **329**, 542–544 (2010).
  - <sup>12</sup> Togan, E., Chu, Y., Imamoglu, A. & Lukin, M. D. Laser cooling and real-time measurement of the nuclear spin environment of a solid-state qubit. *Nature* **478**, 497–501 (2011).
  - <sup>13</sup> Neumann, P. *et al.* Multipartite entanglement among single spins in diamond. *Science* **320**, 1326–1329 (2008).
  - <sup>14</sup> Jiang, L. *et al.* Repetitive readout of a single electronic spin via quantum logic with nuclear spin ancillae. *Science* **326**, 267–272 (2009).
  - <sup>15</sup> Waldherr, G. *et al.* Quantum error correction in a solid-state hybrid spin register. *Nature* **506**, 204–207 (2014).
  - <sup>16</sup> Taminiau, T. H., Cramer, J., van der Sar, T., Dobrovitski, V. V. & Hanson, R. Universal control and error correction in multi-qubit spin registers in diamond. *Nat Nano* **9**, 171–176 (2014).
  - <sup>17</sup> Fischer, R. *et al.* Bulk nuclear polarization enhanced at room temperature by optical pumping. *Phys. Rev. Lett.* **111**, 057601 (2013).
  - <sup>18</sup> Fischer, R., Jarmola, A., Kehayias, P. & Budker, D. Optical polarization of nuclear ensembles in diamond. *Phys. Rev. B* **87**, 125207 (2013).
  - <sup>19</sup> Gali, A. Identification of individual  $c^{13}$  isotopes of nitrogen-vacancy center in diamond by combining the polarization studies of nuclear spins and first-principles calculations. *Phys. Rev. B* **80**, 241204 (2009).
  - <sup>20</sup> Smeltzer, B., McIntyre, J. & Childress, L. Robust control of individual nuclear spins in diamond. *Phys. Rev. A* **80**, 050302 (2009).
  - <sup>21</sup> Steiner, M., Neumann, P., Beck, J., Jelezko, F. & Wrachtrup, J. Universal enhancement of the optical readout fidelity of single electron spins at nitrogen-vacancy centers in diamond. *Phys. Rev. B* **81**, 035205 (2010).
  - <sup>22</sup> Dréau, A., Maze, J.-R., Lesik, M., Roch, J.-F. & Jacques, V. High-resolution spectroscopy of single nv defects coupled with nearby  $^{13}\text{C}$  nuclear spins in diamond. *Phys. Rev. B* **85**, 134107 (2012).
  - <sup>23</sup> Gaebel, T. *et al.* Room-temperature coherent coupling of single spins in diamond. *Nat. Phys.* **2**, 408–413 (2006).
  - <sup>24</sup> Wang, H.-J. *et al.* Sensitive magnetic control of ensemble nuclear spin hyperpolarization in diamond. *Nat. Commun.* **4**, 1–7 (2013).
  - <sup>25</sup> London, P. *et al.* Detecting and polarizing nuclear spins with double resonance on a single electron spin. *Phys. Rev. Lett.* **111**, 067601 (2013).
  - <sup>26</sup> Liu, G.-Q. *et al.* Protection of centre spin coherence by dynamic nuclear spin polarization in diamond. *Nanoscale* **6**, 10134–10139 (2014).
  - <sup>27</sup> Alvarez, G. *et al.* Local and bulk  $^{13}\text{C}$  hyperpolarization in n-centered diamonds at variable fields and orientations. *arXiv*. **1412**, 8635 (2014).
  - <sup>28</sup> King, J. P. *et al.* Room-temperature in situ nuclear spin hyperpolarization from optically-pumped nitrogen vacancy centers in diamond. *arXiv:1501.02897* (2015).
  - <sup>29</sup> Fuchs, G. D. *et al.* Excited-state spectroscopy using single spin manipulation in diamond. *Phys. Rev. Lett.* **101**, 117601 (2008).
  - <sup>30</sup> Doherty, M. W. *et al.* The nitrogen-vacancy colour centre in diamond. *Physics Reports* **528**, 1–45 (2013).
  - <sup>31</sup> Loubser, J. H. N. & van Wyk, J. A. Electron spin resonance in the study of diamond. *Rep. Prog. Phys.* **41**, 1201 (1978).
  - <sup>32</sup> Gali, A., Fyta, M. & Kaxiras, E. *Ab initio* supercell calculations on nitrogen-vacancy center in diamond: Electronic structure and hyperfine tensors. *Phys. Rev. B* **77**, 155206 (2008).
  - <sup>33</sup> Felton, S. *et al.* Hyperfine interaction in the ground state of the negatively charged nitrogen vacancy center in diamond. *Phys. Rev. B* **79**, 075203 (2009).
  - <sup>34</sup> Smeltzer, B., Childress, L. & Gali, A.  $^{13}\text{C}$  hyperfine interactions in the nitrogen-vacancy centre in diamond. *New J. Phys.* **13**, 025021 (2011).
  - <sup>35</sup> Maze, J. R., Taylor, J. M. & Lukin, M. D. Electron spin decoherence of single nitrogen-vacancy defects in diamond. *Phys. Rev. B* **78**, 094303 (2008).
  - <sup>36</sup> Zhao, N., Ho, S.-W. & Liu, R.-B. Decoherence and dynamical decoupling control of nitrogen vacancy center electron spins in nuclear spin baths. *Phys. Rev. B* **85**, 115303 (2012).
  - <sup>37</sup> Cappellaro, P. Spin-bath narrowing with adaptive parameter estimation. *Phys. Rev. A* **85**, 030301 (2012).
  - <sup>38</sup> Abtew, T. A. *et al.* Dynamic jahn-teller effect in the  $\text{nv}^-$  center in diamond. *Phys. Rev. Lett.* **107**, 146403 (2011).
  - <sup>39</sup> Manson, N. B., Harrison, J. P. & Sellars, M. J. Nitrogen-vacancy center in diamond: Model of the electronic structure and associated dynamics. *Phys. Rev. B* **74**, 104303 (2006).
  - <sup>40</sup> Robledo, L., Bernien, H., van der Sar, T. & Hanson, R. Spin dynamics in the optical cycle of single nitrogen-vacancy centres in diamond. *New J. Phys.* **13**, 025013 (2011).
  - <sup>41</sup> Ma, Y., Rohlfing, M. & Gali, A. Excited states of the negatively charged nitrogen-vacancy color center in diamond. *Phys. Rev. B* **81**, 041204 (2010).
  - <sup>42</sup> Choi, S., Jain, M. & Louie, S. G. Mechanism for optical initialization of spin in nv center in diamond. *Phys. Rev. B* **86**, 041202 (2012).
  - <sup>43</sup> Acosta, V. M., Jarmola, A., Bauch, E. & Budker, D. Optical properties of the nitrogen-vacancy singlet levels in diamond. *Phys. Rev. B* **82**, 201202 (2010).
  - <sup>44</sup> Delaney, P., Greer, J. C. & Larsson, J. A. Spin-polarization mechanisms of the nitrogen-vacancy center in diamond. *Nano Lett.* **10**, 610–614 (2010).
  - <sup>45</sup> Togan, E. *et al.* Quantum entanglement between an optical photon and a solid-state spin qubit. *Nature* **466**, 730–734 (2010).
  - <sup>46</sup> Yang, W. & Sham, L. J. General theory of feedback control of a nuclear spin ensemble in quantum dots. *Phys. Rev. B* **88**, 235304 (2013).
  - <sup>47</sup> Yang, W. & Sham, L. J. Collective nuclear stabilization in single quantum dots by noncollinear hyperfine interaction. *Phys. Rev. B* **85**, 235319 (2012).
  - <sup>48</sup> Wang, P., Du, J. & Yang, W. Engineering nuclear spin dynamics with optically pumped nitrogen-vacancy center. *arXiv:1503.00243* (2015).
  - <sup>49</sup> Clerk, A. A., Devoret, M. H., Girvin, S. M., Marquardt, F. & Schoelkopf, R. J. Introduction to quantum noise, measurement, and amplification. *Rev. Mod. Phys.* **82**, 1155–1208 (2010).

- <sup>50</sup> Hanson, R., Mendoza, F. M., Epstein, R. J. & Awschalom, D. D. Polarization and readout of coupled single spins in diamond. *Phys. Rev. Lett.* **97**, 087601 (2006).
- <sup>51</sup> Maurer, P. C. *et al.* Room-temperature quantum bit memory exceeding one second. *Science* **336**, 1283–1286 (2012).
- <sup>52</sup> Greilich, A. *et al.* Nuclei-induced frequency focusing of electron spin coherence. *Science* **317**, 1896–1899 (2007).
- <sup>53</sup> Xu, X. *et al.* Optically controlled locking of the nuclear field via coherent dark-state spectroscopy. *Nature* **459**, 1105–1109 (2009).
- <sup>54</sup> Vink, I. T. *et al.* Locking electron spins into magnetic resonance by electron-nuclear feedback. *Nat. Phys.* **5**, 764–768 (2009).
- <sup>55</sup> Sun, B. *et al.* Persistent narrowing of nuclear-spin fluctuations in inas quantum dots using laser excitation. *Phys. Rev. Lett.* **108**, 187401 (2012).

#### ACKNOWLEDGEMENTS

This work was supported by NSFC (Grant No. 11274036 and No. 11322542) and the MOST (Grant

No. 2014CB848700).

#### AUTHOR CONTRIBUTIONS STATEMENT

W. Y. and P. W. conceived the idea, formulated the theories, analyzed the results, and wrote the paper. All authors discussed the results and the manuscript.

#### ADDITIONAL INFORMATION

Competing financial interests: The authors declare no competing financial interests.